Electronic hybridization effect on 4*f* electron crystal field states of $PrOs_4P_{12}$

Kazuaki Iwasa,* Kotaro Saito, and Youichi Murakami†
Department of Physics, Tohoku University, Sendai 980-8578, Japan

Hitoshi Sugawara
Faculty of Integrated Arts and Sciences, The University of Tokushima, Tokushima 770-8502, Japan
(Received 10 January 2009; revised manuscript received 8 May 2009; published 8 June 2009)

Crystal-field excitation spectra of Pr 4*f* electron state in the filled skutterudite $PrOs_4P_{12}$ measured by inelastic neutron scattering experiment evolve distinctly with temperature variation. The spectral widths of excitations from the ground-state singlet to the two triplets and their temperature dependences are well reproduced by the theory based on the exchange coupling between 4*f* and conduction electrons. The shift of level energies by around 1 meV below 60 K indicates modification of crystal-field potential with variation of thermal population of 4*f* electron crystal-field states. The spectral evolution is consistent with the specific heat data that deviates from the calculated one for the well-localized 4*f* electron. The result supports the effect of *p*-*f* hybridization between Pr 4*f* and P *p* states in $PrOs_4P_{12}$.

DOI: 10.1103/PhysRevB.79.235113 PACS number(s): 71.70.Ch, 71.27.+a, 78.70.Nx

I. INTRODUCTION

Spectroscopy of *f*-electron states has elucidated various physical properties of rare-earth and actinide compounds. Hybridization effect as a consequence of interplay between *f* and conduction electrons in heavy fermion or valence fluctuation systems exhibits quasielastic or broad magnetic-excitation spectra, instead of well-defined crystal-field (CF) excitations of localized *f* electrons.[1] It was theoretically studied on the basis of the degenerate Anderson model, for instance.[2,3] One of extensively studied effect is *p*-*f* hybridization between *f* electrons and *p* holes of the pnictogens, which was introduced in the study of complex magnetic structures of Ce monopnictides.[4] It explains the unexpectedly small CF splitting between a ground state and a excited state, and gives rise to the magnetic polaron ordered state. Recently, the concept of *p*-*f* hybridization also applied to understanding multipolar ordering as well as heavy electrons in rare-earth filled skutterudite.[5–7]

Rare-earth filled skutterudite RT_4X_{12} (R=lanthanide and actinide elements, T=transition metal, and X=pnictogen) crystallizes in the body-centered cubic structure represented by the space group Im $\bar{3}(T_h^5)$.[8] 12 *X* atoms form an icosahedron cage in which *R* ions are located, and the cages are connected by *T* ions. It has been suggested that *p*-*f* hybridization between *R* and *X* atoms plays a role in the various electronic properties and the *p* state predominates the density of states at the Fermi energy.[9] Among them, $PrRu_4P_{12}$ showing a metal-nonmetal transition at T_{M-I}=63 K is a typical system.[10] $LaRu_4P_{12}$ without 4*f* electron does not undergo such charge-density wave (CDW) transition, despite that the very similar Fermi surface as that of $PrRu_4P_{12}$ was verified both theoretically and experimentally.[11] Then the role of 4*f* electrons in the metal-nonmetal transition of $PrRu_4P_{12}$ was investigated by the inelastic neutron scattering experiment. The CF level energies and the spectral widths strongly depend on temperature.[12] The polarized neutron diffraction study concluded that the two inequivalent Pr-ion CF schemes align in staggered way by $\mathbf{q}_0$=(100) below T_{M-I}.[13] Based on the band calculation study, the Fermi surfaces are approximately parallel to the {100} planes bisecting the line between Γ and *X* points.[14] Therefore, this phase transition was interpreted to be a CDW formation owing to a three-dimensional Fermi-surface nesting by $\mathbf{q}_0$. These facts were explained by the scenario of antiferro-type ordering of totally symmetric multipoles of 4*f* electrons, providing a band gap as cooperation with the Fermi-surface nesting condition.[15] Thus, the new type of CDW state originating from the *p*-*f* hybridization effect was established. Recently, the phase transition from heavy electron state to nonmagnetic ordered one in $PrFe_4P_{12}$ at 6.5 K is also explained by the higher-rank antiferro-type ordering of multipoles conserving the local cubic symmetry.[16] Thus the *p*-*f* hybridization effect is generally responsible for the low-temperature electronic properties in Pr-filled skutterudite.

The isostructural material $PrOs_4P_{12}$ does not exhibit any phase transition down to 0.1 K.[17] Recent study on the Fermi surface of this material revealed that the nesting condition with $\mathbf{q}_0$ does not exist[18,19] so that no gap formation occurs and the metallic state is conserved down to the lowest temperature. The specific heat as a function of temperature was not in accordance with the well-localized 4*f* state, which may be a trace of hybridization as was pointed out by Matsuhira *et al.*[20] It is interesting to investigate the hybridization effect on the single Pr-ion state in $PrOs_4P_{12}$ without any phase transition, since this material can show the backbone mechanism of electron correlation. We carried out inelastic neutron scattering experiment to measure the CF excitation spectra of $PrOs_4P_{12}$ and will present characteristic temperature dependence of CF spectra reflecting the strong hybridization effect.

II. EXPERIMENTAL DETAILS

Single-crystalline samples of $PrOs_4P_{12}$ and $LaOs_4P_{12}$ were synthesized by the Sn-flux method in The University of

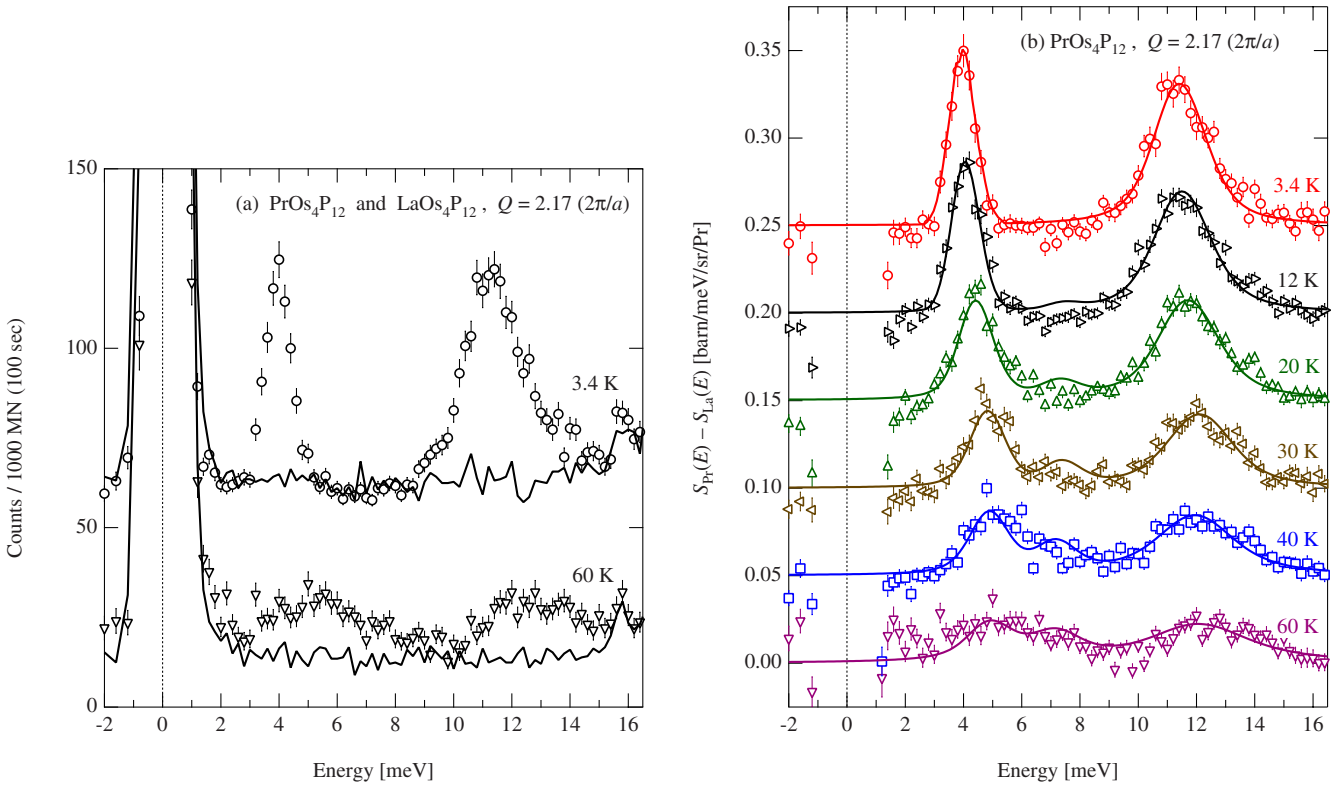

FIG. 1. (Color online) (a) Symbols and lines represent total scattering intensities of $PrOs_4P_{12}$ and $LaOs_4P_{12}$, respectively, measured at 3.4 and 60 K with the fixed scattering vector magnitude $Q=2.17(2\pi/a)$. Ordinate origin of each temperature data is shifted by 50. (b) Symbols represent magnetic scattering function of $PrOs_4P_{12}$ as difference of responses between $PrOs_4P_{12}$ and $LaOs_4P_{12}$. Ordinate origin of each temperature data is shifted by 0.05. Solid lines are results of spectral fitting based on the model for CF splitting.

Tokushima. The sample qualities are basically the same as those used in the de Haas–van Alphen experiments.[18] The samples for neutron scattering experiments were prepared by crashing the single-crystalline ones into powder form weighting 5.0 and 6.9 g of $PrOs_4P_{12}$ and $LaOs_4P_{12}$, respectively. The inelastic neutron scattering experiments were performed at the Tohoku University triple-axis thermal neutron spectrometer TOPAN installed at the beam hole 6G of the research reactor JRR-3, Japan Atomic Energy Agency, Tokai, Japan. The scattered neutron was selected at 13.5 meV by a pyrolytic graphite crystal analyzer. Higher-order contamination was eliminated by a pyrolytic graphite filter installed after the sample. Incident neutron energy, which was also selected by pyrolytic graphite crystals, was changed to perform inelastic scattering measurements. Horizontal collimators were open-60′-60′-60′. The Gaussian-like energy-resolution function has 0.85 meV of full width at half maximum at the elastic scattering condition, determined by incoherent scattering intensity from vanadium. That, at the finite energy transfer of 10 meV, is estimated as 1.4 meV. Sample temperatures were controlled between 3.4 and 60 K by a helium closed-cycle refrigerator.

III. RESULTS AND ANALYSIS

Figure 1(a) shows scattering intensities from $PrOs_4P_{12}$ (symbols) and $LaOs_4P_{12}$ (lines) measured at 3.4 and 60 K. The intensities were normalized by the sample mass. We succeeded in detecting magnetic scattering responses locating around 4 and 11 meV of Pr-based compound. Figure 1(b) shows the temperature dependence of the magnetic response functions $S_{Pr}(E)-S_{La}(E)$, where $S(E)=\frac{1}{N}(\frac{k_f}{k_i})^{-1}\frac{d^2\sigma}{d\Omega dE_f}$ at the fixed scattering vector magnitude of $Q=2.17(2\pi/a)$, where $a=8.080$ Å is a reported lattice constant of $PrOs_4P_{12}$.[17]

These results of $S_{Pr}(E)-S_{La}(E)$ are evaluated by correcting absorption, subtracting the phonon contribution and background intensity estimated from the measurement of $LaOs_4P_{12}$, eliminating the higher-order contamination in the incident monitor counter,[21] and converting the intensity into the scattering function in absolute units based on the incoherent intensity of vanadium standard sample. Distinct magnetic peaks observed at around 4.0 and 11.2 meV are interpreted as excitations between CF levels of Pr^{3+} $4f^2$ electrons as discussed later. With increasing temperature, the peak positions shift apparently to higher-energy side and the spectral widths become broader. The CF energy shift and the spectral broadening were observed also for the metal-nonmental system $PrRu_4P_{12}$,[12] which are enhanced in the nonmetallic multipolar ordered phase with the vanishment of carrier. Thus the temperature variation of the CF excitations of $PrOs_4P_{12}$ can be considered as a characteristic feature of $4f$-electron states interplaying with the carrier.

In order to derive temperature dependences of CF level scheme, we analyzed the observed spectra based on the CF Hamiltonian[22] expressed as

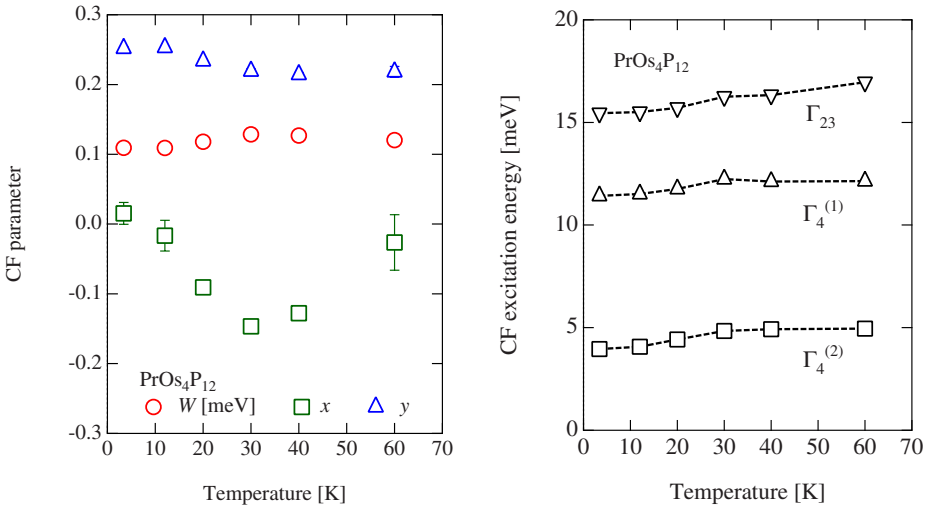

FIG. 2. (Color online) (a) CF parameters in Eq. (1) and (b) CF excitation energies measured from the ground state Γ_1 determined from the least-squares fitting analysis for the data shown in Fig. 1(b).

$$\mathcal{H}_{\mathrm{CF}} = W\left[\frac{x}{F_4}(O_4^0 + 5O_4^4) + \frac{1-|x|}{F_6^c}(O_6^0 - 21O_6^4) + \frac{y}{F_6^t}(O_6^2 - O_6^6)\right], \quad (1)$$

where O_m^n expresses a Stevens' operator equivalent. The last term with y is caused by the lack of the point symmetry C_4 in T_h for the filled skutterudite compounds. We take F_4=60, F_6^c=1260, and F_6^t=30 for Pr^{3+} $4f^2$ state, as defined in the reference. The $4f^2$-electron state of Pr^{3+} splits into four levels; a singlet Γ_1, a nonmagnetic non-Kramers doublet Γ_{23}, and two triplets $\Gamma_4^{(1)}$ and $\Gamma_4^{(2)}$. The magnetic scattering function is proportional to squared magnitude of a transition matrix element between two levels.[23] We calculated CF excitation spectra assumed to be expressed by Lorentzian functions convoluted with the spectrometer resolution expressed by a Gaussian form. A least-squares fitting procedure of the calculation to the experimental data was carried out to evaluate the CF coefficients (W, x, and y) in Eq. (1), a scale factor between the calculated cross-sections and the experimental intensities, and the Lorentzian spectral widths of the two peaks located at around 4.0 and 11.2 meV. The results are shown by solid lines in Fig. 1 reproducing the experimental data well. Another small peak at around 7 meV seen at higher temperature corresponds to the transition between excited states. We assumed the same width for this component as that at 4 meV. The small discrepancy between the calculated and the measured results may indicate that this assumption is not sufficient or that the subtraction of $LaOs_4P_{12}$ data has ambiguity (some data points become actually negative). However, the well reproducibility of the overall spectra supports the validity of the present analysis.

The resultant CF coefficients are plotted against temperature in Fig. 2(a). The sequence of CF levels is $\Gamma_1 - \Gamma_4^{(2)} - \Gamma_4^{(1)} - \Gamma_{23}$ in the whole measured temperature range as shown in Fig. 2(b), which is consistent with the previously reported schemes deduced from the specific-heat data.[20]

The shifts of CF eigenenergies are up to 0.9 meV with varying temperature between 3.4 and 60 K, which is unexpectedly large among $4f$ electron systems.

The intrinsic half-width at half maximum (HWHM) $\gamma(T)$ for the excitation from Γ_1 to $\Gamma_4^{(2)}$ and that from Γ_1 to $\Gamma_4^{(1)}$ are depicted by circles and squares, respectively, in Fig. 3.

Both intrinsic widths increase with increasing temperature as was seen in some metallic rare-earth systems.[1] The thermal broadening phenomenon strongly indicates the exchange interaction between f electrons and carrier. Another attractive feature is that the width of the excitation from Γ_1 to $\Gamma_4^{(1)}$ is much broader than that of the excitation from Γ_1 to $\Gamma_4^{(2)}$, despite that the both triplet states are categorized into the same symmetry. Quantitative analysis for the temperature evolution of the intrinsic widths will be shown in the next section. We will discuss later the effect of the shift of CF levels on the temperature dependence of specific heat that deviates from the calculated one for the temperature-independent definite level splitting.

IV. DISCUSSIONS

The increase of spectral widths of CF excitations was discussed by Becker, Fulde, and Keller (BFK),[24] by taking into

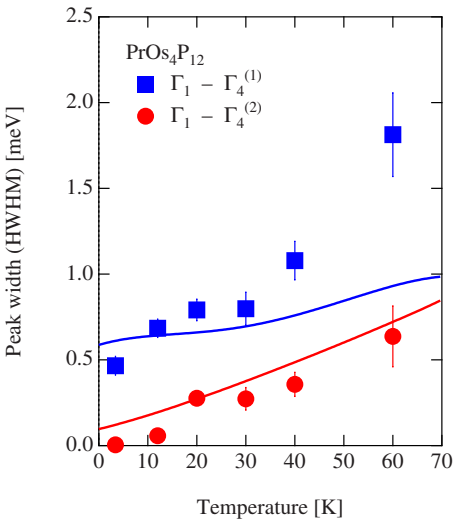

FIG. 3. (Color online) Spectral widths for the excitations $\Gamma_1 - \Gamma_4^{(1)}$ (blue squares) and $\Gamma_1 - \Gamma_4^{(2)}$ (red circles) determined from the least-squares fitting analysis for the data shown in Fig. 1(b).

account the exchange interaction between $4f$ electrons and carrier. They derived a general form of the HWHM $\gamma(T)$ for the CF excitation peak described by a Lorentzian function. They denoted the broadening originating from the damping due to conduction electron-hole excitation. Hereafter, we derive $\gamma(T)$ for the case of $4f^2$ $J=4$ state with the ground-state Γ_1 singlet in T_h space group, following the theoretical argument by BFK.

The BFK theory proposed the calculation of $\gamma(T)$ in case of CF states under O_h symmetry; $\Gamma_1^{(O_h)}$, $\Gamma_4^{(O_h)}$, and $\Gamma_5^{(O_h)}$. On the other hand, in the T_h space group for filled skutterudite compounds $\Gamma_4^{(O_h)}$ and $\Gamma_5^{(O_h)}$ mix with each other. The triplet CF states $\Gamma_4^{(1)}$ and $\Gamma_4^{(2)}$ are represented as

$$|\Gamma_t^{(T_h)},m\rangle = \sqrt{1-d^2}|\Gamma_5^{(O_h)},m\rangle + d|\Gamma_4^{(O_h)},m\rangle, \tag{2}$$

where $|\Gamma_t^{(T_h)},m\rangle$ and $|\Gamma_t^{(O_h)},m\rangle$ express the wave function of triplets denoted by index $m=1,2,3$ for T_h and O_h symmetries, respectively.[25] The coefficient d is determined by the CF coefficients W, x, and y in the CF Hamiltonian (1). Taking $d=0$ and 1 correspond to the triplet $\Gamma_5^{(O_h)}$ and $\Gamma_4^{(O_h)}$, respectively. Adopting this wave-function form and the BFK theory, we derived the intrinsic HWHM for the excitation from Γ_1 to one of the triplet as

$$\gamma(T) = 2\pi[J_{\mathrm{ex}}N(E_F)]^2\left[\frac{40d^2}{3}k_BTe^{-\Delta_{\mathrm{CF}}/k_BT} + \frac{20d^2}{3}\frac{\Delta_{\mathrm{CF}}}{1-e^{-\Delta_{\mathrm{CF}}/k_BT}} + \frac{1}{2}(5-4d^2)^2k_BT\right], \tag{3}$$

where J_{ex} denotes an exchange constant multiplied by g_J-1 between $4f$ and conduction electrons, $N(E_F)$ is the density of states at the Fermi level, and Δ_{CF} is the CF splitting energy. For analyzing the present data, we have to consider two excitations from Γ_1 to $\Gamma_4^{(2)}$ and Γ_1 to $\Gamma_4^{(1)}$, as observed in the present neutron scattering. $N(E_F)$ is assumed to be constant in the whole temperature range, since no distinct anomaly was seen in the electrical resistivity data. The values of Δ_{CF} have already shown in Fig. 2(b). The values of d, which have also been determined in the aforementioned spectral analysis based on Eq. (1), are around 0.81 and 0.59 for $\Gamma_4^{(1)}$ and $\Gamma_4^{(2)}$, respectively. Therefore, the temperature dependences of spectral widths of $PrOs_4P_{12}$ can be fitted by Eq. (3) with a single parameter $J_{\mathrm{ex}}N(E_F)$. The best fit result for HWHM data with the parameter $J_{\mathrm{ex}}N(E_F)=0.0244\pm0.0005$ is shown by the solid lines in Fig. 3. The result is quantitatively consistent with the observation below 30 K, although it deviates from the data in higher-temperature region with worse accuracy due to the less magnetic intensity. We concluded that the intrinsic widths of the singlet-triplet CF excitation spectra are given by the exchange interaction. The origin of the strong exchange interaction is expected to be p-f hybridization as described before. It is notable that the BFK theory agrees with the fact that the width for the excitation to $\Gamma_4^{(1)}$ is larger than that for $\Gamma_4^{(2)}$. It can be understood by the different electron-charge distributions of $\Gamma_4^{(1)}$ and $\Gamma_4^{(2)}$ from each other. The former has extended electron cloud to the neighboring P sites, resulting into overlapping of wave functions between $4f$ and p states. Thus, the damping becomes significant for the excitation to $\Gamma_4^{(1)}$.

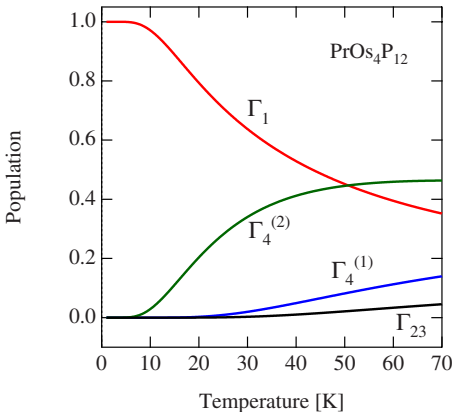

FIG. 4. (Color online) Thermal population probability of the CF levels calculated from the present neutron scattering result shown in Fig. 2(b).

The evolution of CF spectra is also given by coupling with phonon state, for example, splitting of CF quartet excited state in $CeAl_2$ where the coupled optical phonon energy is comparable to the CF splitting energy.[26,27] It should be notable that the broader spectra of the excitation $\Gamma_1-\Gamma_4^{(2)}$ than that of $\Gamma_1-\Gamma_4^{(1)}$ are observed not only in $PrOs_4P_{12}$ but also in $PrOs_4Sb_{12}$ (Refs. 28 and 29) and $PrRu_4Sb_{12}$,[30] despite that phonon state and the CF splitting are not equivalent among the three Pr-based skutterudite compounds. In addition, $PrRu_4P_{12}$ in the nonmetallic phase exhibits sharp CF excitation spectra with the almost same widths for the excitations from Γ_1 to $\Gamma_4^{(1)}$ and to $\Gamma_4^{(2)}$.[12] It means that the electronic interaction is more responsible for the observed broadening and temperature dependence of CF spectra than the phonon effect. Thus, it is validated to apply the general description of the CF excitation width based on the BFK theory to the metallic Pr-filled skutterudite. The detailed analysis for the CF excitation widths of $PrOs_4Sb_{12}$ and $PrRu_4Sb_{12}$ will be published in near future.

The shift of the eigenenergies of CF levels of $PrOs_4P_{12}$ is also a characteristic feature. The CF levels and parameters vary gradually below around 30 K with the certain accuracy as seen in Fig. 2. The temperature 30 K is comparable to the CF splitting energy between the Γ_1 ground state and the $\Gamma_4^{(2)}$ first excited state. We show temperature variations of thermal population probabilities of the CF levels in Fig. 4, calculated from the scheme depicted in Fig. 2(b).

The populations are insensitive against temperature above 40 K. On the other hand, below 30 K, the population probability of the ground state Γ_1 becomes dominant. This fact means that the $4f$ wave function contributing to p-f hybridization changes around 30 K. Therefore, the CF potential given by p-f hybridization is expected to depend on temperature resulting in the shift of the CF splitting energy. The shift of CF levels was also observed for $PrRu_4P_{12}$ below T_{M-I}. It is comprehensive as the variation of effective CF potential with the evolution of ordered $4f$ electron multipoles (totally symmetric hexadecapole and hexacontatetrapole) mediated by the strong p-f hybridization. The observed similarity of

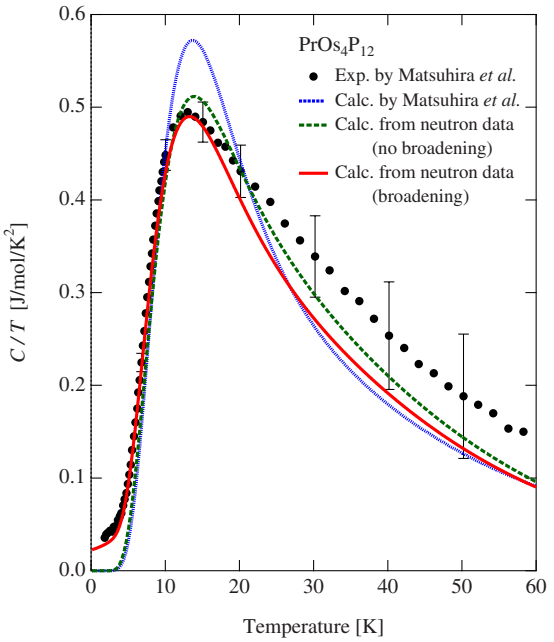

FIG. 5. (Color online) Solid circles represent magnetic specific-heat data quoted from the paper by Matsuhira *et al.* (Ref. 20). A blue dotted line is the calculated one from the fixed CF schemes determined in this specific-heat measurement. A green broken line is obtained from the temperature dependent CF levels determined in the present neutron data without taking into account the broadening of the neutron spectra. A red solid line is that with spectral broadening.

CF level evolution in both compounds indicates a strong electronic interaction due to p-f hybridization in the Pr-filled skutterudite.

The specific heat originating from Pr $4f$ state in $PrOs_4P_{12}$ was reported by Matsuhira *et al.*,[20] which is quoted as solid circles in Fig. 5.

The result is obtained by subtracting the specific heat data of $LaOs_4P_{12}$ predominated by phonon contribution from that of $PrOs_4P_{12}$ so that the error bars in higher-temperature region become larger. One can also expect uncertainty due to contribution of conduction electrons on the Fermi surface. However, examining the effect of characteristic CF splitting to the specific-heat data is meaningful for understanding the electronic properties. They also reported the calculated one for the simple well-localized $4f^2$ state providing the fixed CF splitting scheme of $\Gamma_1-\Gamma_4^{(2)}(48\ \mathrm{K})-\Gamma_4^{(1)}(140\ \mathrm{K})-\Gamma_{23}(180\ \mathrm{K})$, which is shown by a blue dotted line giving the largest value among the calculation in Fig. 5. It is not in accordance with the experimental data satisfactorily. The reason for the discrepancy was proposed to be the electron hybridization. Since the CF splitting energies strongly depend on temperature as observed in the present measurement, we took into account this fact for calculating the specific heat. A green broken line in Fig. 5 is the result based on the temperature-dependent CF levels shown in Fig. 2(b), without taking into account the spectral broadening. This calculation gives better agreement with the experimental data than the temperature-independent CF levels. In order to examine the effect by the spectral broadening, we also calculated the specific heat by considering the spectral broadening in addition to the CF level shift. We assumed that the intrinsic widths of the $\Gamma_4^{(1)}$ and $\Gamma_4^{(2)}$ states are the spectral widths for the each excitations based on the present analysis result expressed by the lines in Fig. 3. We assumed also that Γ_1 had no broadening and Γ_{23} had the same width as $\Gamma_4^{(1)}$. The result is presented by a red solid line in Fig. 5. The calculated C/T and the measured data coincide with each other below 20 K, and the deviation in the temperature range above 20 K is within the experimental error. Therefore, the variation of the CF spectrum due to the p-f hybridization is consistent with the broad Schottky peak of specific heat.

V. SUMMARY

We report that the CF state of $PrOs_4P_{12}$ is determined by the strong electron hybridization effect. The intrinsic widths of the CF excitations from the ground state Γ_1 to the two triplets Γ_4 are well reproduced by the BFK theory taking into account the exchange interaction between f and conduction electrons. The shift of CF level schemes indicates that the f state population change gives rise to the variation of CF potential determined by p-f hybridization. It is also supported by the consistency between the present neutron scattering result and the specific heat. Therefore, we conclude that the strong p-f hybridization is responsible for the electronic properties in $PrOs_4P_{12}$. In contrast to the multipolar ordering systems $PrRu_4P_{12}$ and $PrFe_4P_{12}$, $PrOs_4P_{12}$ without the Fermi-surface nesting condition does not undergo any phase transition.[18] However, the characteristic strong hybridization effect takes place commonly in Pr-filled skutterudite.

ACKNOWLEDGMENTS

This study is partially supported by the Grants-in-Aid for Scientific Research from Ministry of Education, Culture, Sports, Science and Technology, Japan [Scientific Research on Priority Area "Skutterudite" (No. 15072206), Scientific Research (C) (No. 19540355 and No. 20540358), Priority Areas of New Materials Science Using Regulated Nano Spaces (No. 20045008-01), Scientific Research on Innovative Areas "Heavy Electrons" (No. 20102005), JSPS Fellows (No. 20·08728), and Scientific Research (S) (No. 21224048)]. The neutron scattering experiment was performed under the User Program conducted by ISSP, University of Tokyo. A part of the inelastic neutron scattering was performed under the collaboration with R. Igarashi.

*iwasa@m.tains.tohoku.ac.jp
†Present address: Condensed Matter Research Center, Institute of Materials Structure Science, High Energy Accelerator Research Organization, Ibaraki 305-0801, Japan.

[1] E. Holland-Moritz and G. H. Lander, *Handbook on the Physics and Chemistry of the Rare-Earths* (Elsevier Science BV, Amsterdam, 1994), Vol. 19, p. 1.
[2] Y. Kuramoto and E. Müller-Hartmann, J. Magn. Magn. Mater. **52**, 122 (1985).
[3] D. L. Cox, N. E. Bickers, and J. W. Wilkins, J. Magn. Magn. Mater. **54-57**, 333 (1986).
[4] H. Takahashi and T. Kasuya, J. Phys. C **18**, 2697 (1985); **18**, 2709 (1985); **18**, 2721 (1985); **18**, 2731 (1985); **18**, 2745 (1985); **18**, 2755 (1985).
[5] J. Otsuki, H. Kusunose, and Y. Kuramoto, J. Phys. Soc. Jpn. **74**, 200 (2005).
[6] J. Otsuki, H. Kusunose, and Y. Kuramoto, J. Phys. Soc. Jpn. **74**, 2082 (2005).
[7] Y. Kuramoto, Prog. Theor. Phys. Suppl. **176**, 77 (2008).
[8] B. C. Sales, *Handbook on the Physics and Chemistry of Rare-Earths* (Elsevier Science BV, Amsterdam, 2003), Vol. 33, p. 1.
[9] H. Harima and K. Takegahara, J. Phys.: Condens. Matter **15**, S2081 (2003).
[10] C. Sekine, T. Uchiumi, I. Shirotani, and T. Yagi, Phys. Rev. Lett. **79**, 3218 (1997).
[11] S. R. Saha, H. Sugawara, Y. Aoki, H. Sato, Y. Inada, H. Shishido, R. Settai, Y. Ônuki, and H. Harima, Phys. Rev. B **71**, 132502 (2005).
[12] K. Iwasa, L. Hao, K. Kuwahara, M. Kohgi, S. R. Saha, H. Sugawara, Y. Aoki, H. Sato, T. Tayama, and T. Sakakibara, Phys. Rev. B **72**, 024414 (2005).
[13] K. Iwasa, L. Hao, T. Hasegawa, T. Takagi, K. Horiuchi, Y. Mori, Y. Murakami, K. Kuwahara, M. Kohgi, H. Sugawara, S. R. Saha, Y. Aoki, and H. Sato, J. Phys. Soc. Jpn. **74**, 1930 (2005).
[14] H. Harima and K. Takegahara, Physica B (Amsterdam) **312-313**, 843 (2002).
[15] T. Takimoto, J. Phys. Soc. Jpn. **75**, 034714 (2006).
[16] A. Kiss and Y. Kuramoto, J. Phys. Soc. Jpn. **75**, 103704 (2006).
[17] W. M. Yuhasz, P.-C. Ho, T. A. Sayles, T. Yanagisawa, N. A. Frederick, M. B. Maple, P. Rogl, and G. Giester, J. Phys.: Condens. Matter **19**, 076212 (2007).
[18] H. Sugawara, Y. Iwahashi, K. Magishi, T. Saito, K. Koyama, H. Harima, D. Kikuchi, H. Sato, T. Endo, R. Settai, and Y. Ônuki, Phys. Rev. B **79**, 035104 (2009).
[19] H. Harima and K. Takegahara, Physica B (Amsterdam) **403**, 906 (2008).
[20] K. Matsuhira, Y. Doi, M. Wakeshima, Y. Hinatsu, K. Kihou, C. Sekine, and I. Shirotani, Physica B (Amsterdam) **359-361**, 977 (2005).
[21] G. Shirane, S. M. Shapiro, and J. M. Tranquada, *Neutron Scattering with a Triple-Axis Spectrometer* (Cambridge University Press, Cambridge, England, 2002), p. 117.
[22] K. Takegahara, H. Harima, and A. Yanase, J. Phys. Soc. Jpn. **70**, 1190 (2001); **70**, 3468 (2001); **71**, 372 (2002).
[23] R. J. Birgeneau, J. Phys. Chem. Solids **33**, 59 (1972).
[24] K. W. Becker, P. Fulde, and J. Keller, Z. Phys. B **28**, 9 (1977).
[25] R. Shiina, J. Phys. Soc. Jpn. **73**, 2257 (2004).
[26] M. Loewenhaupt, B. D. Rainford, and F. Steglich, Phys. Rev. Lett. **42**, 1709 (1979).
[27] P. Thalmeier and P. Fulde, Phys. Rev. Lett. **49**, 1588 (1982).
[28] K. Kuwahara, K. Iwasa, M. Kohgi, K. Kaneko, N. Metoki, S. Raymond, M.-A. Méasson, J. Flouquet, H. Sugawara, Y. Aoki, and H. Sato, Phys. Rev. Lett. **95**, 107003 (2005).
[29] E. A. Goremychkin, R. Osborn, E. D. Bauer, M. B. Maple, N. A. Frederick, W. M. Yuhasz, F. M. Woodward, and J. W. Lynn, Phys. Rev. Lett. **93**, 157003 (2004).
[30] D. T. Adroja, J.-G. Park, E. A. Goremychkin, N. Takeda, M. Ishikawa, K. A. McEwen, R. Osborn, A. D. Hillier, and B. D. Rainford, Physica B (Amsterdam) **359-361**, 983 (2005).